DESIGN OF MAGNETS FOR AN OPEN-SECTOR CYCLOTRON

H.N. Jungwirth, L.D. Bruins, A.H. Botha and J.L. Pabot

Council for Scientific and Industrial Research, Pretoria, South Africa.

Abstract

An open-sector cyclotron (OSC) with a maximum proton energy of 200 MeV has been proposed as the main stage of a national accelerator facility for the Republic of South Africa. Solid-pole cyclotrons are envisaged as injectors for a wide range of ions. The basic requirements for the magnets of the OSC are given and considerations which influence their design are outlined. Methods which have been developed to analyse the design of OSC magnets in terms of orbit properties are described. Characteristics of the magnets are given. For more detailed beam dynamical investigations realistic magnetic fields are determined by numerical methods and used for orbit integration. Results obtained in this way are presented. The reliability of computed fields is established by comparing calculated with measured results for a test magnet.

1. Introduction

The basic requirements for the proposed OSC in terms of the whole facility are outlined in another paper of this conference[1]. For design considerations of the magnets they can be summarised as follows: (i) variable proton energy from 20 to 200 MeV; (ii) ion range up to ^{84}Kr with the possibility of enhancing the K-factor for heavy ions; (iii) total energy gain of approx. 25; (iv) high beam intensities for lighter ions; (v) compatibility with injectors.

It was shown by M.M. Gordon[2] and verified in the IUCF[3] that a separated-sector field (no spiralling) of periodicity N=4 can supply strong vertical beam focusing in this energy range with a relatively simple magnet system. Only this field type was therefore considered in our design. However, the following paragraph is kept more general for its wider application potential.

2. Analysis of Orbit Properties in OSC Fields

Focusing properties and requirements for isochronism in magnet configurations of the separated-sector type are well-known in hard-edge field models[2]. The fact that they quite often change considerably in realistic fields can be attributed mainly to the influence of the edge field.

2.1 Step-edge Field Model

An analytical solution of this problem requires a field model which allows a simple construction of equilibrium orbits (e.o.) and yields simple formulas. This can be achieved by assuming a stepwise field change in the edge region of the pole gap and such a field model is therefore called a step-edge field. Of the various possibilities for approximating a realistic edge field distribution in this way, the one which was chosen to replace the hard-edge model is shown in Fig. 1.

The width of the edge region w can be related to simple design parameters of a magnet. With a slight empirical adjustment w is given by:

$$w = 2{,}4(g + e + s) \qquad (1)$$

The meaning of these parameters is shown in Fig. 1. If the iron edge cannot be defined as indicated, the sum of e and s must be replaced by an equivalent single parameter.

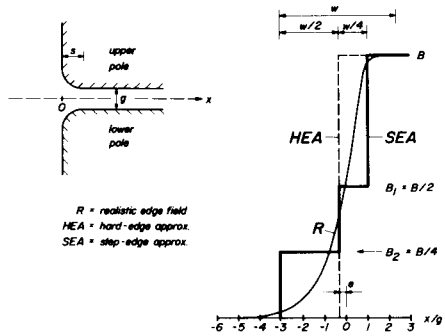

Fig. 1: Stepwise approximation of a realistic edge field

2.2 Orbit Geometry and Isochronism

As can be confirmed analytically the total angle of deflection φ for an ion crossing the step region is the same as in the part of the hard-edge field which it replaces. The significant part of the e.o. in the two field models is shown in Fig. 2.

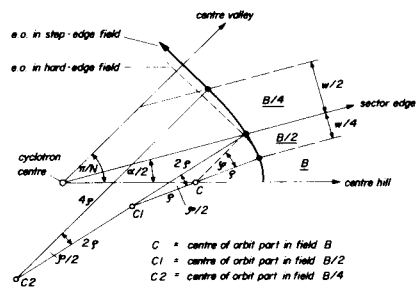

Fig. 2: Geometry of equilibrium orbits in a step-edge field

Geometrical relations indeed become very simple. In comparison with the hard-edge e.o. only one additional parameter, φ, has to be introduced and is given by:

$$\varphi = \pi/N - \alpha/2 + \arcsin[w/(4\rho) - \sin(\pi/N - \alpha/2)] \qquad (2)$$

N is the number, α the angular width and ρ the orbit radius in the field region B of the magnet sectors. The parameter ρ is equal to the one which is used in hard-edge and w is given by eqn. (1).

One can see that for a constant w the value of φ decreases with increasing ρ. The properties of e.o. in a step-edge field change, therefore, for different radial positions. The step-edge field

Proc. 7th Int. Conf. on Cyclotrons and their Applications (Birkhäuser, Basel, 1975), p. 193-196

model fails as soon as the argument of the arcsin becomes larger than 1. This can be used in practice to determine the lower limit of a convenient injection energy.

The equation which governs the requirements for an isochronous field can be written as:

$$B = (m_o/q)\ (1/\rho)\nu\gamma \qquad (3)$$

where m_o and q are the rest mass and charge of the ion, ν is the orbit frequency, γ the relativistic mass increase factor and l the length of the e.o. For the hard-edge case l is given by:

$$l_{HE} = 2N\rho[\pi/N+\sin(\pi/N)\sin(\pi/N-\alpha/2)/\sin(\alpha/2)] \qquad (4)$$

The term $(1/\rho)$ in (3) is therefore constant for a given N and α. In order to keep ν constant B simply has to be proportional to γ. For the orbit length in the step-edge field one can deduct:

$$l_{SE} = l_{HE}+4N\rho[\varphi-\sin\varphi-2\sin^2(\varphi/4)\sin(\varphi/2)] \qquad (5)$$

The basic mechanism which causes the edge field to increase the orbit length becomes geometrically obvious in Fig. 2. Since φ is changing with ρ the term $(1/\rho)$ is changing in a step-edge field with constant w, and B must be adjusted for isochronism to compensate for the increased value of $(1/\rho)$. This results in a shift of the isochronous e.o. towards smaller radii within the magnet sector.

2.3 Approximate Betatron Frequencies

Since the e.o. in a step-edge field is known, approximate values for the horizontal (radial) and vertical betatron frequencies ν_x, ν_z can be determined analytically. For this purpose an integration method by L.C. Teng[4] including second order terms was used. Results which were obtained in this way for the hard-edge field compared very well over a wide range of α and energies with the exact ones published by M.M. Gordon[2].

Due to their considerable length the second order formulas can be used in practice only in a computer program and are omitted here. Instead, only the first order results for the step-edge field are given which correspond to the so-called 'smooth-approximation' formulas in hard-edge. They are:

$$\nu_x^2 = \alpha_m, \quad \nu_z^2 = [1-5N\varphi/(8\pi)]\ (f+1) - \alpha_m \qquad (6)$$

where α_m is the momentum compaction defined by:

$$\alpha_m = \frac{R}{p(R)}\ \frac{dp(R)}{dR}$$

with $R = l/2\pi$ (l = orbit length), p = particle momentum. The parameter f is the hard-edge flutter which is given in smooth-approximation by:

$$f = (N/\pi)\sin(\pi/N)\sin(\pi/N-\alpha/2)/\sin(\alpha/2) \qquad (7)$$

If the step-edge field has been made isochronous according to equations (3) and (5) α_m becomes equal to γ^2. In this case ν_x assumes the value γ as for hard-edge, but is valid for a smaller ρ.

The formula for ν_z clearly shows the decreasing influence of the edge-field and describes the realistic behaviour very well. It should be noted that not only is the flutter alone affected by edge considerations, but actually the whole positive term (f+1). In all circumstances where α_m is a slowly changing function of ρ, the change of ν_z will be determined by the first term rather than by the second one. This condition can be found near injection, for low energy lighter ions and for all heavy ions.

3. Design Considerations

Compatibility with solid-pole cyclotrons as injectors, for a wide range of ions and energies favours a magnet design featuring rather low orbit frequencies in the OSC and 6,5 MHz was found to be a convenient value for the fastest particle (protons of 200 MeV at extraction). This results in an average radius of approx. 1 m at injection for the required energy gain in the OSC which leaves enough space in the central region to accommodate injection elements. It also allows a relatively large orbit separation at extraction. The four magnets can be kept within reasonable dimensions.

With a harmonic number of 4 the RF range is limited to a maximum of 26 MHz. Assuming peak acceleration in delta resonators an upper limit of approx. 38° is imposed on the choice of the magnet angle α. This value coincides with the situation for which it becomes difficult to avoid crossing the $\nu_z = 1$ resonance.

The lower limit for a possible choice of α is given by $\nu_z = 2$ (N/2 stop band). With feasible values of w it can be expected to occur at around 22° and by decreasing α further the heaviest ions will first be excluded from acceleration. However, a choice of 22° would result in a maximum field of approx. 2,05T in our case. Considerations with respect to the field shape in the pole gap of OSC magnets[5,6] make it advisable to avoid field values above 1,5T if the magnets are used over a wide excitation range. This limits the choice of α to values larger than 28°. Alternatively, either one would have to decrease the orbit frequency further which leads to larger and less economic magnets or field trimming becomes rather difficult.

A survey of beam-dynamical properties over the remaining range of α was made. The method which has been outlined in the previous paragraph was used with a design value of 32 cm for w. It has been found that α-values from 30° to 32° cannot be used, because the working path for high proton energies in the $\nu_z - \nu_x$ diagram runs for a large energy range along the $2\nu_z + \nu_x = 4$ coupling resonance. Design values of 29° and 33° seemed feasible, but were also dismissed. The first because ν_z hovers around the 3/2 half-integer resonance for proton energies in the region near 80 MeV where high-intensity beams are required, 33° because below the same energy range one gets close to $2\nu_z + \nu_x = 4$ again.

In order to remain at a safe distance from this resonance as well as from the $\nu_z = 1$ resonance a value of 34° has been chosen. Results for this angle are shown in Fig. 3. Curves for heavier ions are the same as those for proton energies with an equivalent relativistic mass increase.

These results indicate that passing through

the $\nu_z = \nu_x$ resonance cannot be avoided in our design and must be studied.

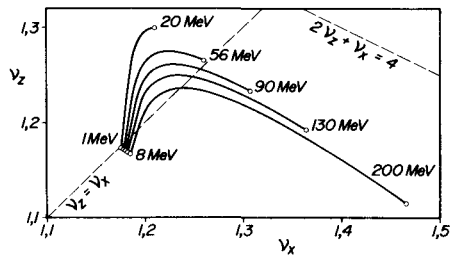

Fig. 3: Approximate focusing properties for various proton energies in the chosen magnet design with N = 4, α = 34° and w = 32 cm as parameters.

4. Magnet Properties

The magnet system comprises four identical C-magnets of which one is shown in Fig. 4. The pole tips are separated by a constant gap of 6 cm. The yoke is subdivided into 6 pieces so as to keep the mass of the heaviest part below 50t and to simplify manufacturing and assembling. The pole tips, but preferably also the yoke parts, must be made from forged or hot-rolled iron bars of high soft-magnetic quality.

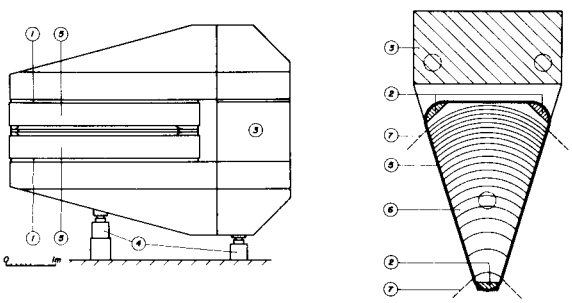

Fig. 4: Side view (a) and cross-section (b) of a single sector magnet comprising (1) pole tips (2) distance pieces for pole gap (3) yoke parts (4) supporting legs (5) main excitation coils (6) trim-coil sheets (7) equilibrium orbits at injection and extraction.

The chosen machine parameters require a maximum field of 1,27T at extraction and determine the radial position and size of the pole tips. Over a radial distance of approx. 3,4 m the field must increase by 20 % if protons are accelerated to 200 MeV, but has to remain nearly constant for heavy ions. Continuous variation between these two extreme shapes is required for maximum excitation.

Following the method which is used in the OSC magnets of the IUCF[3] field production is therefore distributed between two different coil types. As indicated in Fig. 4 the main field up to 1,15T will be supplied by coils which are wound in a single layer around the pole tips. Such a design decreases as much as possible the additional flux which must be carried by the pole tips. Calculations have shown than an increase of approx. 10 % can be expected relative to the flux density in the pole gap assuming infinite permeability of the iron. At such low flux-density levels saturation effects in the pole tips should be small. For stabilising the position of the effective field boundary the edges of the pole tips towards the valleys are rounded off with a radius of 6 cm.

The required radial field gradient for isochronism will be produced by current sheets which are mounted onto the pole faces. Their geometry is also indicated in Fig. 4. Field is added in the direction of the extraction radius and subtracted in the direction of the injection radius as this method doesn't increase the flux load in the return path. At the same time the power loss in the connecting leads can be decreased considerably by closing half of the current loops around the injection side of the pole tips. In addition also the required space for these leads is decreased by a factor of 2. Each set of trim-coil pairs in the 4 magnets will be powered by a separate supply.

The size of the magnets is kept comparatively small by decreasing the area of the cross-section in the return path in relation to the pole area. The average flux density in the yoke parts is increased in this way to a maximum of 1,55T. Under these conditions the reluctance of the yokes is approx. 10 % of the gap reluctance for a high quality iron. The following table summarizes the main properties of the magnets.

Table: Main design properties of the magnet system

Number of magnets	4
Magnet angle, degr.	34
Magn. flux density in gap (extraction), T	0,38 to 1,27
Magn. flux density in yoke (average), T	0,50 to 1,55
Distance cycl. centre to pole tips, m	0,67
Radial extent of pole tips, m	3,82
Height of magnets, m	4,3
Overall diameter, m	13
Total mass of iron, t	1350
Gap width, mm	60
Max. MMF, At	6×10^4
Number of windings per magnet	50
Power of main supply, kW	350
Trim-coil pairs per magnet	20
Total trim-coil power, kW	50

5. Results for Computed Fields

When magnet angles of 29° and 33° seemed a feasible choice analytical results were checked by numerical orbit integration in realistic fields for protons of 200 MeV extraction energy. Magnet geometries very similar to that in Fig. 4 were used for field computation. The magnets were positioned such that effective field boundaries in the azimuthal direction coincided with radial lines. The iron was assumed to have infinite permeability in these specific cases and a continuously changing current density in the trim-coil sheets provided the theoretically required radial field gradient for isochronism.

Fig. 5 shows the computed field for the 29°-design in a three-dimensional plot. Field values in the median plane are plotted along radial and azimuthal lines at intervals of 1° and 74 mm. The maximum field is 1,47T which yields an orbit frequency of 6,54 MHz.

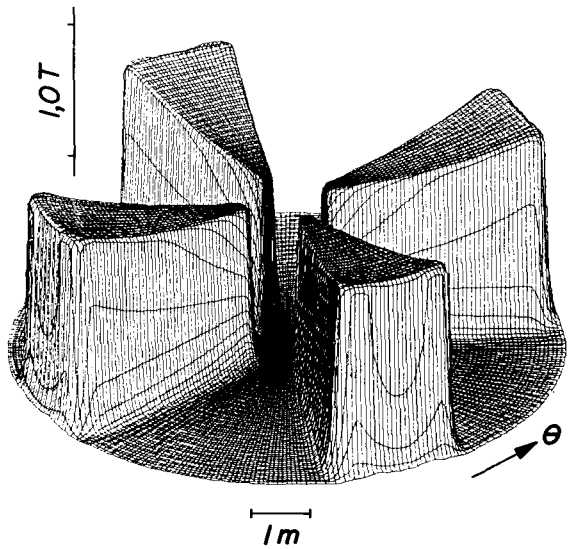

Fig. 5: Computed magnetic field for an OSC with N = 4, α = 29° and a proton energy of 200 MeV

Equilibrium orbits for different energies are isochronous within ± 0,1 % in such fields except in the fringe areas near injection and extraction where the revolution time increases up to 0,6 %. The results for betatron frequencies are shown in Fig. 6. The comparison with analytical values in step-edge approximation establishes the reliability of this model. The effect of the fringe areas on focusing properties can be noticed.

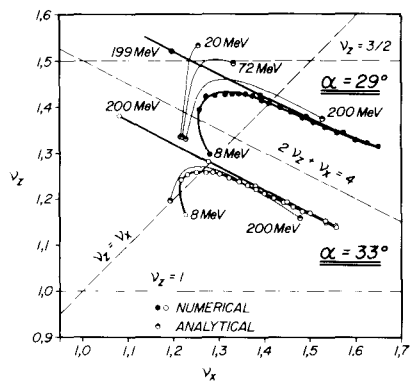

Fig. 6: Focusing properties for a proton beam in realistic magnetic fields with N = 4 and α = 29° as well as 33°

6. Test of Field Computation Method

Computed fields are compared with measurements in a test magnet which is shown in Fig. 7(a). The pole tips are shaped like the radial section of a sector with an angular width of 36° and field values of more than 1,5T can be obtained in the pole gap of 30 mm.

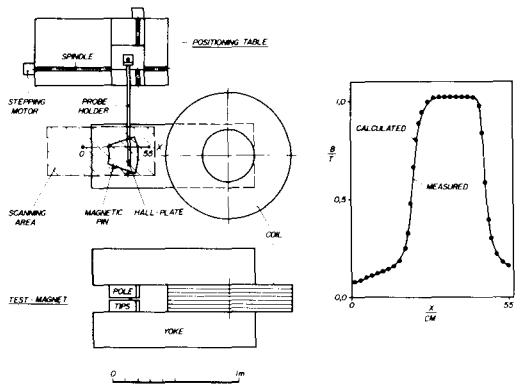

Fig. 7: Magnet (a) for comparing computed with measured fields and a typical result (b)

The field is measured pointwise with an accuracy of ± 3G using an NMR-calibrated Hall-plate (SVB 525) which is temperature stabilized to 0,01°. Positioning and measurements as well as probe orientation are computer controlled. The position of the electrical centre of the Hall-plate can be determined to ± 0,02 mm with respect to the pole geometry. Two demountable pairs of 'magnetic pins' produce distinct field maxima which are directly used to determine the scanning co-ordinates.

Over the whole excitation range computed field values were approx. 4 % lower than those which were measured for the same coil current, probably due to using too low permeability values in the computation. However, as is shown in Fig. 7(b) relative comparisons for equal field values in the pole gap are quite satisfying. With increasing excitation, flux differences of not more than 0,5 % were observed over the measured area. This is caused to a large extent by local iron saturation in the sharp corners and edges of the pole tips.

References

1. W.L. Rautenbach, paper B.21 of this conference.
2. M.M. Gordon, Annals Phys., 50, 571 (1968).
3. M.E. Rickey, 6th Int. Cycl. Conf. AIP Conf. Proc. No. 9, (AIP, New York, 1972), p. 1.
4. L.C. Teng, Rev. Sci. Instr., 27, 12, 1052 (1956).
5. R.E. Pollock, 6th Int. Cycl. Conf. AIP Conf. Proc. No. 9, (AIP, New York, 1972), p. 69.
6. D.L. Friesel and R.E. Pollock, IEE Trans. Nucl. Sci., NS-22, 3, 1891 (1975).